

Photometric observations of Southern Abell Cluster Redshifts Survey Clusters: Structure of galaxies in the inner region of clusters of galaxies

Valeria Coenda¹, Hernan Muriel¹, Carlos José Donzelli¹

Grupo de Investigaciones en Astronomía Teórica y Experimental, IATE, Observatorio Astronómico, Universidad Nacional de Córdoba, Laprida 854, X5000BGR, Córdoba, Argentina.

vcoenda@oac.uncor.edu, hernan@oac.uncor.edu, charly@oac.uncor.edu

Hernan Quintana, Leopoldo Infante

Departamento de Astronomía y Astrofísica, Pontificia Universidad Católica, Vicuña Mackenna 4860, Casilla 306 Santiago 22, Chile.

hquintana@astro.puc.cl, linfante@astro.puc.cl

and

Diego García Lambas¹

Grupo de Investigaciones en Astronomía Teórica y Experimental, IATE, Observatorio Astronómico, Universidad Nacional de Córdoba, Laprida 854, X5000BGR, Córdoba, Argentina.

dgl@oac.uncor.edu

ABSTRACT

We analyze photometric properties of 1384 cluster galaxies as a function of the normalized distance to cluster center. These galaxies were selected in the central region ($r/r_{200} \leq 0.8$) of 14 southern Abell clusters chosen from the Southern Abell Cluster Redshifts Survey (SARS). For 507 of these galaxies we also obtained their luminosity profiles. We have studied the morphology-clustercentric distance relation on the basis of the shape parameter n of the Sérsic's law. We also have

¹Consejo Nacional de Investigaciones Científicas y Técnicas (CONICET), Avenida Rivadavia 1917, C1033AAJ, Buenos Aires, Argentina.

analyzed the presence of a possible segregation in magnitude for both, the galaxy total luminosity and that of their components (i.e. the bulge and the disk).

Results show a marginal (2σ level) decrease of the total luminosity as a function of normalized radius. However, when bulges are analyzed separately, a significant luminosity segregation is found (3σ and 2σ for galaxies in projection and member galaxies respectively). The fraction of bulges brighter than $M_B \leq -22$ is three times larger in the core of clusters than in the outer region. Our analysis of the disk component suggests that disks are, on average, less luminous in the cluster core than at $r/r_{200} \sim 0.8$. In addition, we found that the magnitude-size relation as a function of r/r_{200} indicates (at 2σ level) that disks are smaller and centrally brighter in the core of clusters. However, the Kormendy relation (the bulge magnitude-size relation) appears to be independent of environment.

Subject headings: galaxies: clusters: general — surveys

1. Introduction

It is well known that environment affects galaxy properties as: morphology, luminosity, color, star formation rate, gas content and structure of the subsystems. Different mechanisms have been proposed to explain how these properties can be affected by the environment. A large number of galaxies can be well represented by two major components, the bulge and the disk. These two components can be affected in many ways when the galaxy is moving into the environment of a rich cluster. Moore et al.(1998) follow the evolution of disks galaxies in a rich cluster (galaxy harassment) and find that the result of close encounters is a transformation from disks to spheroids. Fujita and Nagashima (1999) suggested that ram pressure stripping (Gunn and Gott 1972, Abadi et al. 1999) increases the bulge to disk luminosity ratio B/D of normal spiral galaxies due to the suppression of the star formation and hence favoring the transformation into earlier Hubble types.

Luminosity segregation was detected by Rood & Turnrose (1968), Quintana (1979), Capelato et al. (1980), Yepes et al. (1991) and Kashikawa et al. (1998). Moreover, this effect was detected when galaxies are considered through their clustercentric distances or their velocity dispersions (most luminous galaxies have smaller velocity dispersion) (Rood et al. 1972, Biviano et al. 1992). However, luminosity segregation have also found opponents like Noonan (1961), Bahcall (1973) and Sarazin (1980), who suggested that evidences for luminosity segregation are spurious, and mostly due to poor background subtraction. However, his optimized fitting procedure was applied to the Coma cluster data with little background data.

In this paper we analyze the relations between galaxy structure and photometric parameters vs. cluster’s environment. Domínguez et al. (2001) found that parameters defined as a function of the distance to the cluster centre are the most appropriated to represent the morphological segregation of galaxies in the inner relaxed region of nearby clusters. Since the present work concentrates on that region of clusters ($r < r/r_{200}$), we analyze the galaxy properties as a function of the clustercentric distance normalized to r_{200} . Redshift confirmed members and galaxies seen in projection are analyzed separately. The goal of this paper is to quantify the environment dependence of the structural and photometric properties of galaxies in clusters. Our sample consists of 507 galaxies in 14 southern Abell clusters of the SARS sample (Way et al. 2005, Hereafter Paper I). The structural and photometric parameters were obtained in Coenda et al. (2005, Hereafter Paper III). The paper is structured as follows: observations and photometric analysis are described in section 2. In section 3 we derive and analyze our results, and the conclusions are given in section 4.

2. Sample, observations and luminosity profiles

Our sample consists of Cousins R CCD images of 14 Abell clusters with $cz < 40000 km s^{-1}$ corresponding to the Southern Abell Clusters Redshifts Survey (SARS, Paper I). The images were taken with the Swope 1.0 m telescope at Las Campanas Observatory, Chile. The pixel scale was $0.61''$ and the field covers a $20.8'$ square area. The seeing conditions were very similar for the whole sample of clusters. The mean seeing was $2.00''$ and the dispersion 0.18 . Therefore, we believe that our sample is free of any effect due to variations in the seeing conditions. Additional details on the observations and data reduction are given in Paper III. Table 1 lists the cluster sample, their coordinates, velocity dispersions and radial velocities taken from Muriel et al. (2002, Hereafter Paper II). From the listed clusters we have finally analyzed a total of 1384 galaxies (CS1 sample) of which 345 have known redshifts (CS2 sample) (Paper I). Of the 345 with measured redshifts, 313 are cluster members (CS3 sample). Of the 1384 galaxies, 507 have luminosity profiles determined (CS4 sample) and 232 of these galaxies have measured redshifts (CS5 sample), and of these 232, 207 are cluster members (CS6 sample). Luminosity profiles were obtained using the *ellipse* routine within STSDAS (Jedrzejewski, 1987) and were fitted using the standard B + D law:

$$I(r) = I_e \exp \left[-7.688 \left[\left(\frac{r}{r_e} \right)^{1/4} - 1 \right] \right] + I_0 \exp \left(-\frac{r}{r_0} \right) \quad (1)$$

The first term corresponds to the bulge component, being I_e the effective intensity and r_e the effective radius defined as the radius that encloses half of the total luminosity of the bulge. The second term corresponds to the disk component, being I_0 the central intensity

and r_0 the length scale. In addition, we have also used the Sérsic law (Sérsic 1968) to fit the galaxy luminosity profiles:

$$I(r) = I_s \exp\left(-\left(\frac{r}{r_s}\right)^n\right) \quad (2)$$

In this equation I_s is the central intensity and r_s the length scale. The exponent n is a shape parameter, where $n = 0.25$ correspond to the de Vaucouleurs law (de Vaucouleurs 1948) and $n = 1$ correspond to the exponential law (Freeman 1970). Further details on the fitting procedure and error sources can also be seen on Paper III.

3. Results and Discussion

3.1. Selection effects

In this work we aimed to determine the presence of possible correlations between galaxy photometric parameters and cluster global properties. Particularly, we focused our study on the morphological and magnitude segregation through radial correlations. This is justified from the expectations that different physical processes are likely to operate at different radii, thus looking for trends with radius are clearly appropriate if one is trying to understand why we see luminosity and morphological segregations in clusters. In order to avoid systematic effects we have analyzed the sample completeness as well as projection and selection effects. To study the magnitude segregation we must be sure that our sample is free of any radial bias in the galaxy selection. Since SARS does not represent a magnitude complete sample (see Paper I for a more detailed discussion) we have investigated the possible presence of a radial bias between the SARS target selection and apparent magnitude of the galaxies. We analyzed the radial distribution of the quotient between the number of galaxies with known redshifts and the total number of galaxies in a total-magnitude-complete sample (CS1 sample) (limited at $m_t = 18.5$). The analysis was done for three different intervals of the total apparent magnitude m_t (bulge + disk). As can be appreciated in Figure 1 (a) the fraction of bright galaxies with measured redshift present a slight increment towards the central inner region of clusters. In order to avoid any possible bias in our analysis, we have randomly selected a new sample that is free of this bias. We proceeded as follow: randomly selected galaxies with known redshifts were discarded until the fraction of galaxies with redshift as a function of r is nearly constant. This procedure was applied on each of the selected magnitude intervals. Figure 1 (b) shows the resulting galaxy distributions. As a consequence of this procedure we have a new sample with 345 galaxies with measured redshifts (CSC1 sample).

Once the the sample is free of any bias in the redshift selection function, the redshift

information can be used to quantify the fraction of galaxies that are cluster members as a function of the normalized radius and apparent magnitude. This information will be used to correct for projection effect the sample of galaxies without redshift estimates. In order to quantify this projection effect, and using the sample of galaxies free of the redshift selection bias (CSC1 sample), we computed the ratio between the number of redshift-confirmed members and the total number of galaxies with known redshift as a function of a normalized radius. This ratio was computed for both, the total sample and for different intervals of total apparent magnitude (Figures 2 (a) and 2 (b) respectively). Each galaxy without redshift is weighted depending on the clustercentric distances and the total apparent magnitude.

The previous analysis was carried out to study the total luminosity segregation. On the other hand, to study the bulge-disk luminosity segregation we performed a similar analysis considering a subsample of galaxies with luminosity profiles in which profile decomposition was possible.

In order to correct for the magnitude limit, we first determined the luminosity function of the nearest cluster for both all galaxies in projection and for those redshifts-confirmed member galaxies. The obtained luminosity functions were then fitted with the Schechter’s function. These fittings were used to correct the observed galaxy counts according to Whitmore et al. 1993. The same procedure was applied to the analysis of the bulge and the disk systems.

Since we were also interested in the study of the morphological segregation, we have analyzed both completeness and projection effects for those galaxies where we could trace out the luminosity profile. This analysis is similar to the others mentioned above. However, in this case we have considered different intervals of the Sérsic profile parameter n .

3.2. Morphological Segregation

We have adopted for our analysis the cluster characteristic radius, r_{200} . This radius is defined as the radius where the mean inner density is $200\bar{\rho}(z)$. Carlberg et al. (1997) derive a correlation between r_{200} and the cluster mean velocity dispersion (σ):

$$r_{200} = \frac{\sqrt{3}\sigma}{10H(z)} \quad (3)$$

The values of σ used in this work are those quoted in Paper II and the corresponding values of r_{200} can be found in its Table 1.

As it was pointed out in the introduction, the morphology-environment relation of galaxies in clusters has been extensively studied (Dressler 1980, Witmore et al. 1993, Dominguez

et al. 2001). However, in this work we wanted to analyze the mentioned relation in an alternative way using the n parameter which has two major advantages, it is a continuous index and it can be easily reproduced. In order to study the possibility of n being a rough morphology indicator we have explored the n values fitted to those galaxies with different types of luminosity profiles. In Fig. 3 we have plotted the n distribution for those galaxies having pure de Vaucouleur profiles, B + D profiles and pure exponential profiles. The fourth group includes those galaxies for which we could not fit any of the previous functions. It is clearly observed that those galaxies with $r^{1/4}$ luminosity profiles have values of $n < 0.4$. On the other hand, those galaxies with typical B + D profiles show $0.4 < n < 0.7$, while disk galaxies show $0.7 < n < 1.2$. Finally, we have observed that those galaxies with $1.2 < n$ are mostly dwarf ellipticals.

In figure 4 we can observe the correlation between n and r/r_{200} . The left panel corresponds to all galaxies in the sample corrected for projection effects whereas the results shown in the right panel are computed for redshift-confirmed members and corrected for completeness as it was explained in section 3.1. The comparison between the results shown in both panels gives information about the bias introduced by projection effects. As expected, we found that galaxies with low values of n , which roughly correspond to early type galaxies, dominate the central cluster region. We also found that the fraction of early type galaxies increases when the clustercentric distance decreases. Although the behavior in the mentioned panels are similar, the signal is stronger when redshift-confirmed members are considered. Error bars in this and following figures were estimated using the boot-strap re-sampling technique.

3.3. Segregation in Magnitude

We are interested in studying a possible magnitude segregation in clusters. Solanes et al. (1989) used the mean magnitude to test possible dependencies of magnitudes as a function of the projected local density. Probably, one of the best options is the computation of the luminosity function at different clustercentric radii or densities. Nevertheless, this option requires a huge amount of galaxies. An alternative option consists in the computation of the fraction of galaxies brighter than a certain value as a function of the clustercentric radius.

In order to evaluate a possible segregation in magnitude, we have considered three possible parameters: the total absolute magnitude, the bulge magnitude and the disk magnitude. Figure 5 plots the fraction of galaxies with $M_t \leq -21$ as a function of r/r_{200} , using the CS1 sample and CS3 sample. The threshold magnitude was selected in order to have two sub-samples of similar size. It can be observed that galaxy total luminosity marginally (two

sigma level) decreases as a function of r/r_{200} for redshift-confirmed members of the nearest seven clusters (panel (b)). On the other hand, panel (a) shows all galaxies of the previous seven clusters (solid circles) and all cluster galaxies (open circles) respectively. In this case, both samples were corrected for projection effects. However, we can not see a clear correlation between M_t and r/r_{200} .

The study of the bulge sub-system is particularly important since it is a fundamental component of a high fraction of galaxies and seems to have some properties that are independent of the morphological type of the host galaxy. Figure 6 shows the fraction of galaxies with $M_B \leq -22$ versus the clustercentric distance, panels (a) and (b). We can see that bulge luminosity decreases as r/r_{200} increases in all cases. The sample (CS4 sample and CS6 sample) used in this analysis is complete up to $m_t = 18.5$ and therefore it is not necessary complete in bulge magnitude. For this reason, we repeated the previous analysis selecting a bulge-magnitude-complete subsample (CS7 sample). Assuming an euclidian geometry and an uniform space distribution, the function $N_{dot} * 10^{0.6m_b}$ provides a good estimate of the magnitude completeness. We found that our bulge sample is approximately complete up to $m_b = 16.5$. The results can be seen in panels (c) and (d) of Fig. 6. Analogously, we also found a clear correlation between bulge luminosity and r/r_{200} . In these last two cases, we have considered only two bins for statistical reasons.

As it was discussed in the introduction, disks can be seriously affected by several processes when they move close to the center of massive clusters of galaxies. Figure 7 shows, for the same sample of Fig.6, the fraction of galaxies with $M_D \leq -20.5$ as a function of r/r_{200} . It can be observed a clear dependence of M_D with the clustercentric distance (disks become brighter as the clustercentric distance increases). It should be noted that the effect can not be clearly appreciated when all clusters in projection are considered (open circles in panel b).

As it was detailed in Paper III our sample galaxies were selected under a strong restriction: only those galaxies with apparent radius greater than 3-4 times the FWHM were chosen. This selection avoid any bias in the accuracy of measuring bulge and/or disk luminosities. Several tests described in Paper III show that the main error source for the photometric parameters is background noise and an eventual dependence on the bulge and/or disk luminosity should not be noticeable in terms of the calculated errors.

3.4. Scaling Relations

In paper III, we have studied several scaling relations between photometric and structural parameters. In order to test whether these relations depend on the cluster environment, we have correlated their behavior as a function of the over-density radius. We have studied the magnitude-size relation, which is closely related to the Kormendy relation (Kormendy 1977) for bulge systems. Figure 8 shows the $M_B - \log(r_e)$ (panel a) relation together with the $M_D - \log(r_0)$ relation (panel b) for member galaxies. We have separately analyzed this scaling relations for those galaxies with $r/r_{200} < 0.3$ (filled circles) and for those with $r/r_{200} \geq 0.3$ (open circles). The best fitting parameters are shown in the corresponding panels, the slopes and zero points correspond to the bisector fit as described in Paper III. No statistically significant difference between bulges in the inner and in the outskirts part of the clusters was found.

On the other hand, our results indicate a marginal dependency (two σ level) of the $M_D - \log(r_0)$ relation on environment. We can observe from panel (b) of Fig. 8 that for low values of $\log(r_0)$ disks located in the inner cluster regions are brighter than those at intermediate distances from the cluster center. This result implies that the central intensity of disks I_0 would be greater for galaxies located in the inner cluster region. Nevertheless, more data are required in order to confirm this result.

4. Conclusions

We have analyzed the correlation between galaxy photometric parameters and the normalized clustercentric radius r/r_{200} for 507 galaxies in the central region of 14 Abell cluster. All the analysis performed in this work were applied to two different samples: i) all galaxies in projection, for which we have taken into account the standard corrections, and ii) redshift confirmed members corrected by completeness.

Based on the Sérsic index n we analyzed the morphological- r/r_{200} relation. We found that the n parameter is a good alternative to measure the morphological segregation. The use of n has the advantage that it is a continuous parameter that can be estimated in a more reproducible procedure.

In order to test for a possible luminosity segregation, we analyzed the correlation between the fraction of galaxies with $M_t \leq -21$ and r/r_{200} . Our results show a marginal (two sigma level) decrease of the total luminosity as the normalized radius increases. It should be noted that this effect is only present when redshift-confirmed members are considered. The same analysis was repeated for bulge and disk sub-systems. Our results indicate a segre-

gation in bulge-magnitude when both confirmed members galaxies (2σ level) and projected galaxies (3σ level) are used. We found that the fraction of bulges brighter than $M_t \leq -22$ is approximately three times larger in the inner cluster region than in the outer cluster region. This analysis was performed for a total-magnitude-complete sample and for a bulge-magnitude-complete sub-sample. In both cases, our results are consistent with a segregation in the bulge luminosity.

On the other hand, the absolute magnitude of disks presents a dependence on r/r_{200} in the sense that disks tend to have on average lower luminosities as they are closer to the core of the parent cluster of galaxies. It should be noted that this effect is only present when redshift-confirmed members are considered.

If disk galaxies are selected in projection, the effect is only statistically significant for the nearest clusters. Disk luminosity segregation support the idea that disks are tidally affected by the cluster potential or by high speed encounters with other cluster member galaxies. However, there are other phenomena that could affect star formation in galaxy disks such as ram pressure, gas evaporation, or lack of gas accretion from the intra-cluster medium. All these mechanisms can also be responsible for the observed disk luminosity segregation.

We have analyzed the scaling relations for bulges and disks as a function of r/r_{200} . We did not find any statistically significant dependence of the $M_B - \log(r_e)$ relation with the clustercentric distance. Our results suggest that the physical conditions responsible for the Kormendy relation are sufficiently robust to support the extreme conditions found in the core of the clusters of galaxies. On the other hand, the $M_D - \log(r_0)$ relation is consistent with a marginal dependency (two sigma level) of this relation as a function of the normalized radius. The correlation between these two parameters appears weaker in the cluster core when compared with larger clustercentric distances. This result indicates that disks of galaxies in the central region of clusters are more compact and have a brighter central luminosity. Nevertheless, it should be remembered that, on average, disks are less luminous in the central region than in the outskirts. In summary, disks in the core of clusters are less luminous, more compact and present a higher central surface brightness. The simulations performed by Moore et al. (1999) indicate that galaxy harassment is particularly strong for low surface brightness galaxies, which suggests that disks that can survive in the cluster core are the most compact ones, a scenario that is consistent with our results.

Finally, it is important to notice that for most of the analysis made in this work the results clearly differ depending on whether redshift-confirmed members or galaxies in projection are considered. This indicates the importance of using redshift confirmed members.

5. Acknowledgments

This work was partially supported by the Consejo de Investigaciones Científicas y Técnicas de la República Argentina, CONICET; SeCyT, UNC, Agencia Nacional de Promoción Científica and Agencia Córdoba Ciencia, Argentina. L. Infante and H. Quintana acknowledge partial support from the Centro de Astrofísica FONDAP/CONICYT program.

REFERENCES

- Abadi, M. G., Moore, B., & Bower, R. G. 1999, MNRAS, 308, 947
- Bahcall, N. A. 1973, ApJ, 183, 783
- Biviano, A., Girardi, M., Giuricin, G., Mardirossian, F., & Mezzetti, M. 1992, ApJ, 396, 35
- Capelato, H. V., Gerbal, D., Salvador-Sole, E., Mathez, G., Mazure, A., & Sol, H. 1980, ApJ, 241, 521
- Carlberg, R. G., Yee, H. K. C., & Ellingson, E. 1997, ApJ, 478, 462
- Coenda, V., Donzelli, C. J., Muriel, H., Quintana, H., Infante, L., & Lambas, D. G. 2005, AJ, 129, 1237, Paper III
- de Vaucouleurs, G. 1948, Annales d’Astrophysique, 11, 247
- Domínguez, M., Muriel, H., & Lambas, D. G. 2001, AJ, 121, 1266
- Dressler, A. 1980, ApJ, 236, 351
- Freeman, K. C. 1970, ApJ, 160, 811
- Fujita, Y., & Nagashima, M. 1999, ApJ, 516, 619
- Gunn, J. E., & Gott, J. R. I. 1972, ApJ, 176, 1
- Jedrzejewski, R. I. 1987, MNRAS, 226, 747
- Kashikawa, N., Sekiguchi, M., Doi, M., Komiyama, Y., Okamura, S., Shimasaku, K., Yagi, M., & Yasuda, N. 1998, ApJ, 500, 750
- Kormendy, J. 1977, ApJ, 218, 333
- Moore, B., Lake, G., & Katz, N. 1998, ApJ, 495, 139
- Moore, B., Lake, G., Quinn, T., & Stadel, J. 1999, MNRAS, 304, 465
- Muriel, H., Quintana, H., Infante, L., Lambas, D. G., & Way, M. J. 2002, AJ, 124, 1934, Paper II
- Noonan, T. 1961, PASP, 73, 212
- Quintana, H. 1979, AJ, 84, 15

- Rood, H. J., & Turnrose, B. E. 1968, ApJ, 152, 1057
- Rood, H. J., Page, T. L., Kintner, E. C., & King, I. R. 1972, ApJ, 175, 627
- Sarazin, C. L. 1980, ApJ, 236, 75
- Sérsic, J. L. 1968, Atlas de Galaxias Australes, Observatorio Astronómico de Córdoba
- Solanes, J. M., Salvador-Sole, E., & Sanroma, M. 1989, AJ, 98, 798
- Way, M., Quintana, H., Infante, L., Lambas, D. G., Muriel, H. 2005. AJ accepted, Paper I
- Whitmore, B. C., Gilmore, D. M., & Jones, C. 1993, ApJ, 407, 489
- Yepes, G., Dominguez-Tenreiro, R., & del Pozo-Sanz, R. 1991, ApJ, 373, 336

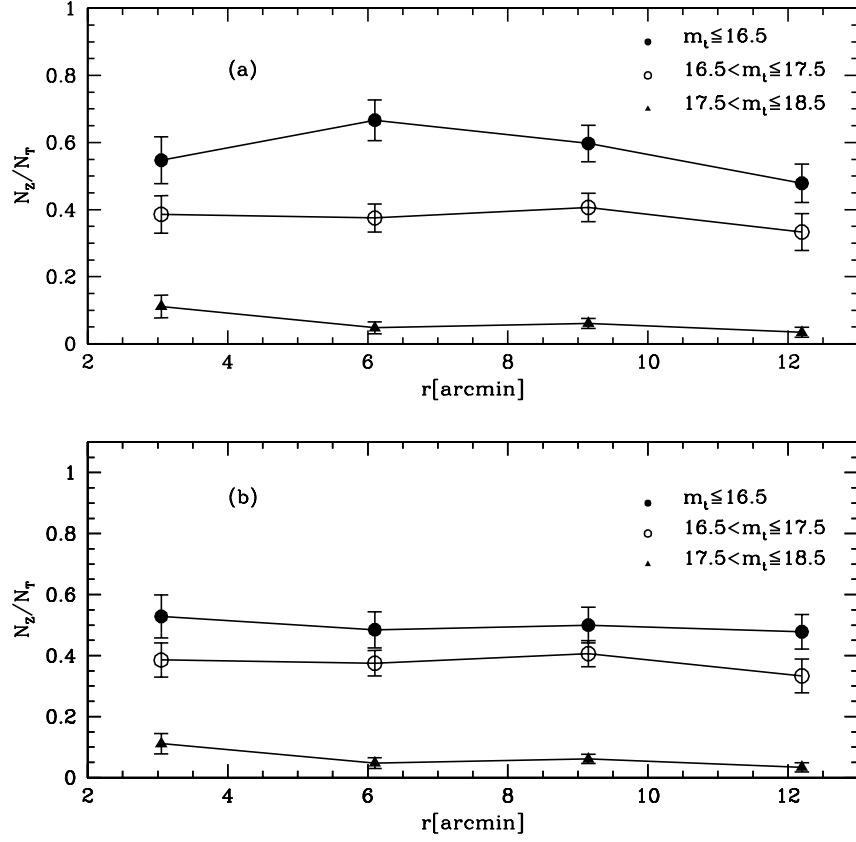


Fig. 1.— (a) Radial distribution of the ratio between the number of galaxies with known redshifts and the total number of galaxies with a limit magnitude at $m_t = 18.5$, on each of the selected magnitude intervals. (b) Same as (a) but bias corrected.

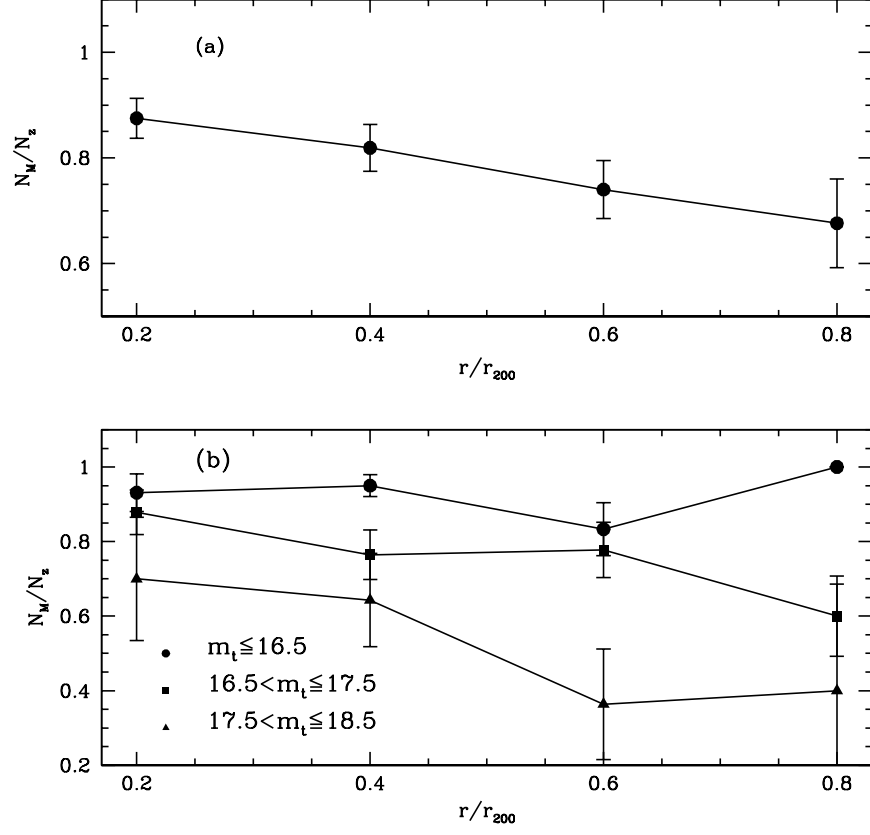


Fig. 2.— Ratio between the number of redshift-confirmed members and the total number of galaxies with known redshifts as a function of r/r_{200} (a) for the total sample and (b) for different magnitude interval.

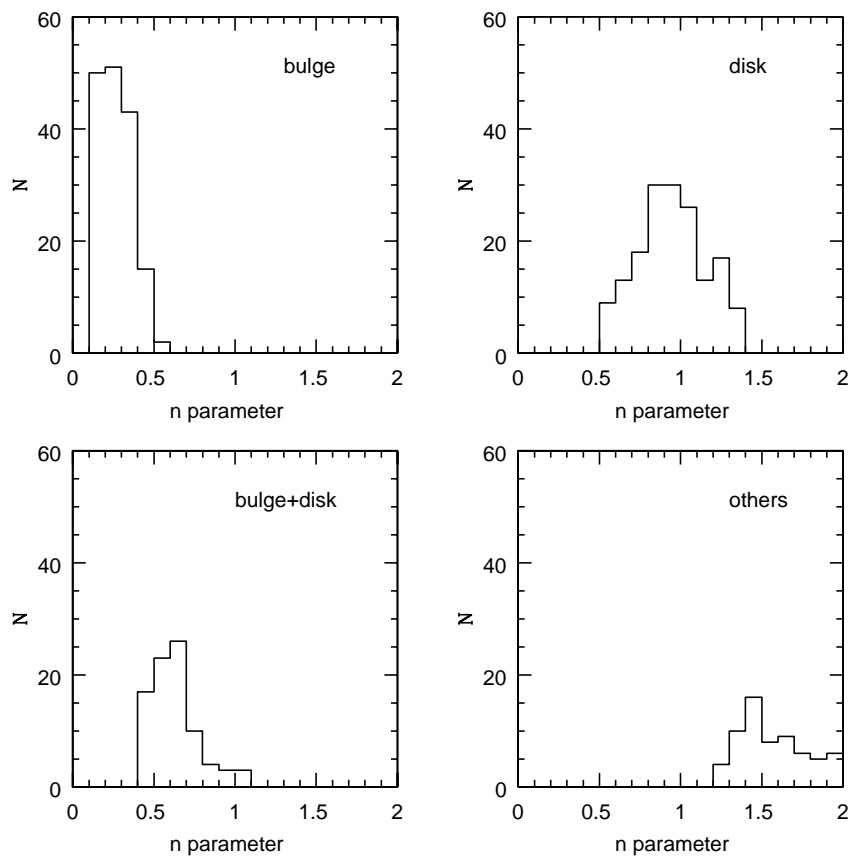


Fig. 3.— Distribution of the n parameter for galaxies having pure de Vaucouleurs profiles, B + D profiles, pure exponential profiles, and galaxies for which we could not fit any of the previous functions.

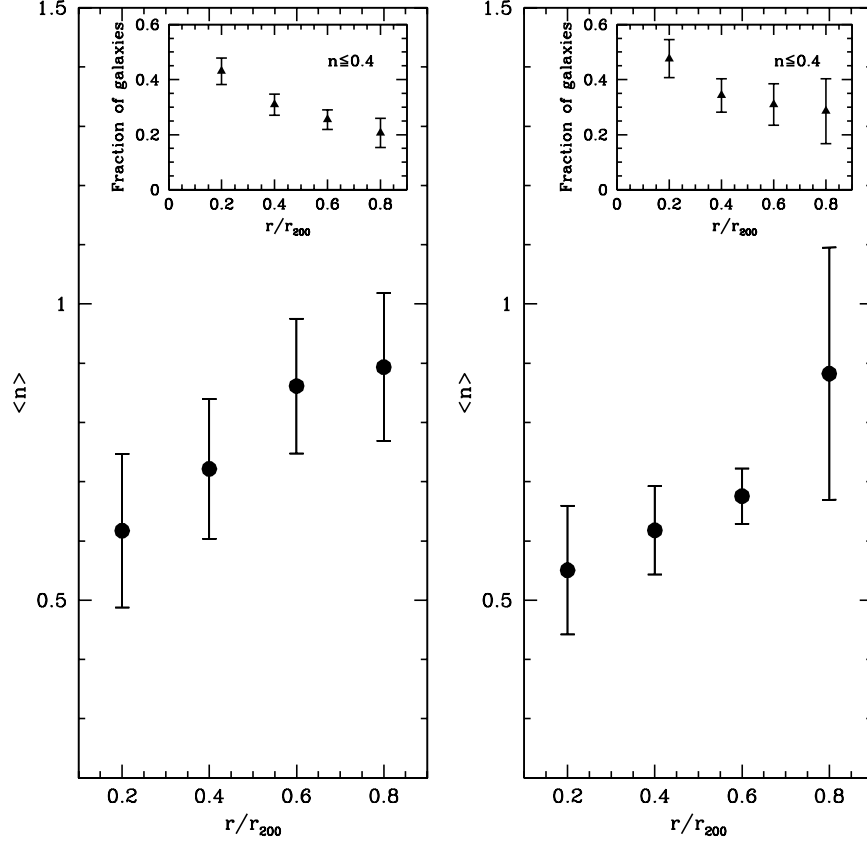


Fig. 4.— Correlation between the average n parameter and normalized clustercentric distance for the sample galaxies, projection corrected (left panel) and confirmed cluster members (right panel). The small box in the upper corner displays the fraction of galaxies with $n \leq 0.4$ as function of r/r_{200} .

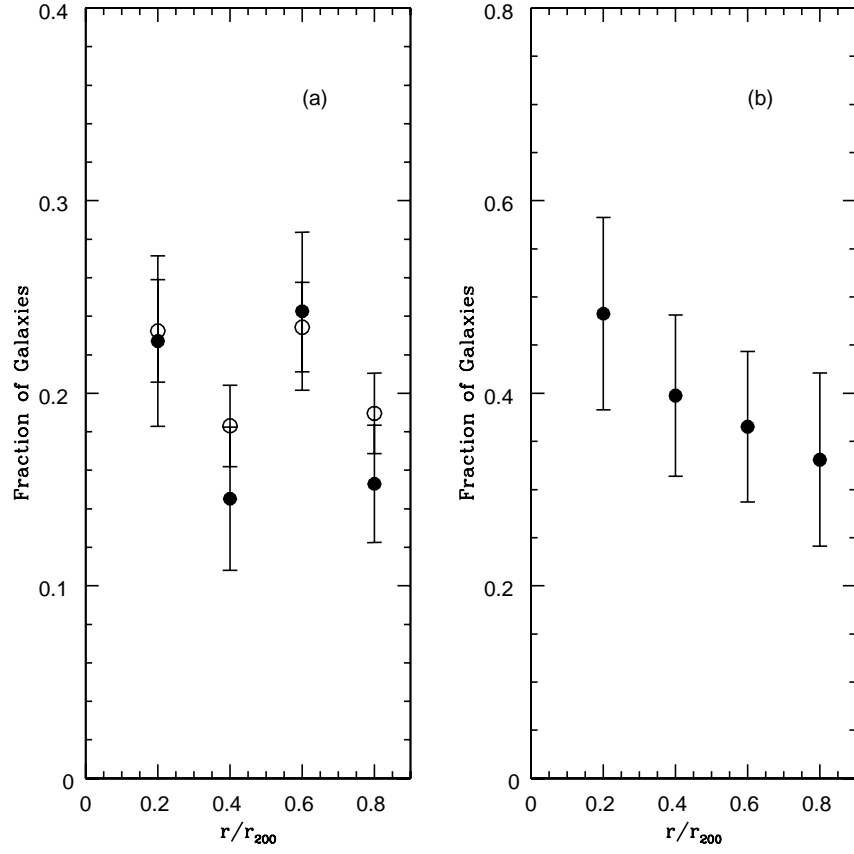


Fig. 5.— Fraction of galaxies with $M_t \leq -21$ as function of r/r_{200} . (a) for all galaxies of the seven nearest clusters (solid circles) and total sample galaxies (open circles) both corrected for projection effects. (b) for redshift-confirmed members of the seven nearest clusters.

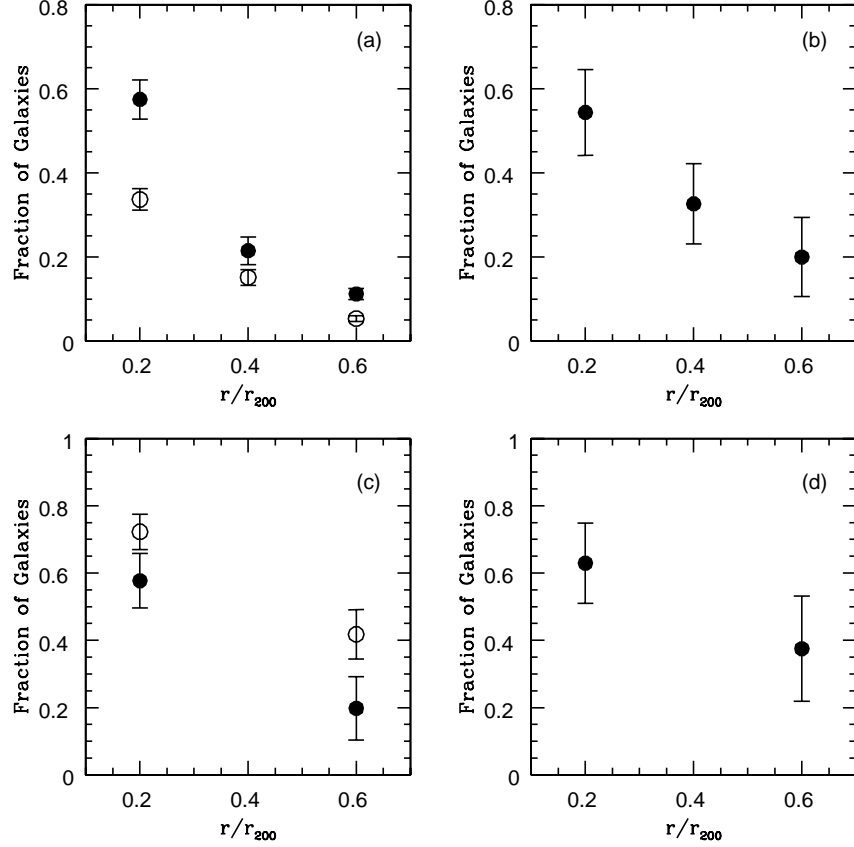


Fig. 6.— Panels (a) and (b) show the fraction of galaxies with $M_B \leq -22$ as function of r/r_{200} for the same sample galaxies of Fig. 5. Panels (c) and (d) show the fraction of galaxies with $M_B \leq -22$ as function of r/r_{200} but in this case limited to a bulge-magnitude-complete subsamples.

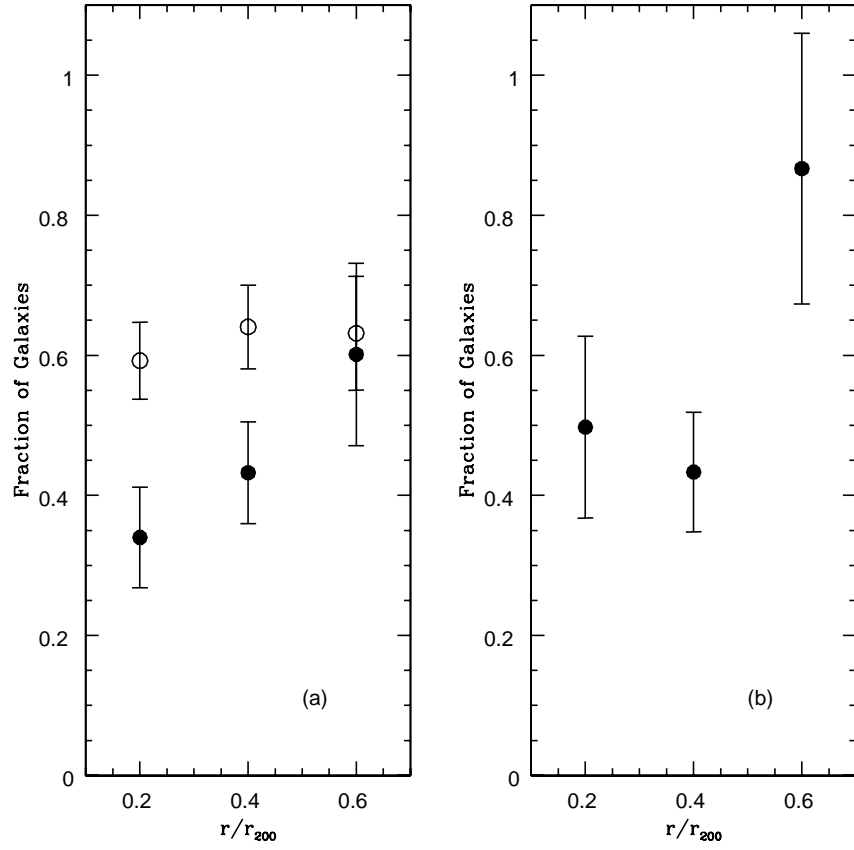


Fig. 7.— Fraction of galaxies with $M_D \leq -20.5$ as function of r/r_{200} . Panels (a) and (b) correspond to the same cases of Fig. 5.

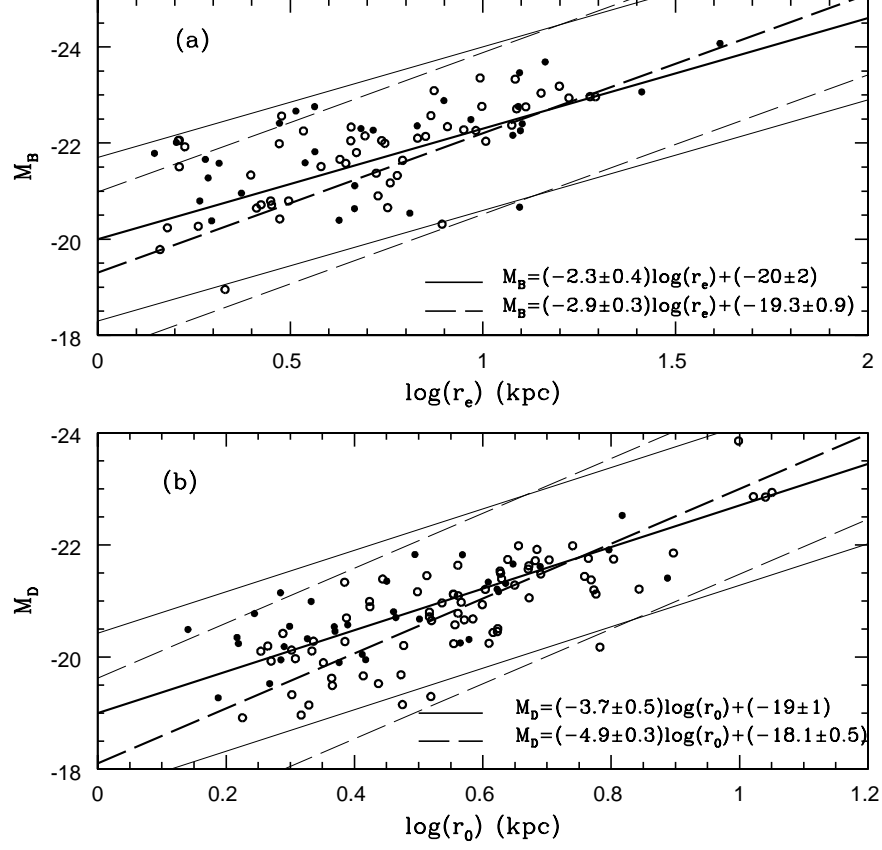


Fig. 8.— $M_B - \log(r_e)$ (a) and $M_D - \log(r_0)$ (b) relation. In both cases, galaxies with $r/r_{200} < 0.3$ are represented with filled circles and the bisector fit is shown with a solid line. Galaxies with $r/r_{200} \geq 0.3$ are plotted with open circles and the bisector fit is shown with a dashed line.

Table 1. Observed clusters

Abell Number	α_{J2000} <i>h m s</i>	δ_{J2000} <i>° ' "</i>	σ [<i>kms</i> ⁻¹]	v_r [<i>kms</i> ⁻¹]
118	00 55 43.9	−26 24 46	669 ± 127	34421 ± 159
2734	00 11 20.1	−28 52 52	784 ± 124	18502 ± 100
2799	00 35 3.00	−39 25 29	563 ± 62	19454 ± 127
2800	00 37 58.7	−25 05 30	335 ± 64	18943 ± 47
2854	01 00 48.7	−50 31 51	308 ± 44	18480 ± 51
2923	01 32 18.0	−31 05 36	670 ± 76	21420 ± 135
2933	01 40 41.2	−54 33 26	759 ± 72	27709 ± 105
3764	21 26 1.00	−34 47 39	795 ± 123	22714 ± 110
3809	21 49 51.7	−43 52 55	560 ± 67	18785 ± 81
3864	22 30 14.4	−52 28 38	847 ± 188	30699 ± 161
3915	22 47 37.0	−52 03 09	815 ± 102	28925 ± 105
3921	22 49 38.6	−64 23 15	788 ± 111	27855 ± 105
4010	23 31 10.3	−36 30 26	743 ± 140	28766 ± 149
4067	23 58 48.3	−60 38 39	738 ± 442	29643 ± 181